

The triple catalytic action of tertiary nitrogen catalysts in recyclable epoxy-anhydride thermosets

Erik G. Rognerud,^{1,‡} Ryan W. Clarke,^{1,‡} J. Bennett Addison,¹ Brandon C. Knott,¹ Natalie J. Schultz,² Silvia Pezzola,³ Alexandra Stovall,¹ Laura K. Dunham¹, Lisa Stanley,¹ Andrea L. Baer,¹ Nicholas A. Rorrer^{1,*}

1. Renewable Resources and Enabling Sciences Center, National Renewable Energy Laboratory, Golden CO, 80401 USA
2. Center for Integrated Mobility Sciences, National Renewable Energy Laboratory, Golden CO, 80401 USA
3. Department of Chemical Science and Technologies, University of Rome Tor Vergata, 00133 Rome, Italy.

‡ Denotes equal contribution

* Corresponding author emails: nicholas.rorrer@nrel.gov

Abstract. The thermosetting polymer matrix in fiber reinforced composites are an important component for energy related applications, such as the lightweighting of vehicles or their use in wind and waterpower turbine blades, due to their ability to provide superior adhesion, stiffness and applicability to a wide range of manufacturing processes. Despite these benefits, today's thermosets are widely considered to be unrecyclable and thus there is a large interest in redesigning these materials to be inherently recyclable such that energy intensive production of fibers and monomers can be circumvented, bolstering composite manufacture supply chains. Polyester covalent adaptable networks (PECANs) are one such promising alternatives to the incumbent, non-recyclable, epoxy-amine thermosets. PECANs can be formed from the ring-opening co-polymerization (ROCOP) of epoxy-anhydride monomer mixtures and subsequent curing at mild temperatures to exhibit similar performance to conventional epoxies but also possessing unique dynamic chemistries along the ester-hydroxyl backbone that are capable of transesterification and thus reprocessability. While significant advancements have been made in formulating these materials for improved mechanical properties, or optimizing solvolysis and reprocessing strategies, less attention has been placed on the impact of the residing amine catalyst used to generate the polyester network. In this work we evaluated the triple-catalytic efficacy of 12 tertiary amines that act as a curing (bulk ROCOP), a transesterification (internal bond exchange), and a deconstruction (methanolysis) catalyst for PECAN thermosets. Specifically, we first distinguish chain-growth and step-growth polymerization mechanisms for epoxy-amine and epoxy-anhydride mechanisms. We also utilized density functional theory (DFT) to estimate the basicity (pK_b) of each catalyst. Of the tested catalysts, the ROCOP of the studied PECAN network can be completed between 95 minutes and 247 minutes (at 80 °C), with variable gelation phenomenon. Additionally, the stress relaxation (transesterification metric) efficiency of the tested PECAN networks with alternative embedded catalysts ranged from 95% to 15% reduction in stress after 5 hours at 200 °C and the depolymerization efficacy ranged from 2.5% to 9.8% deconstruction after 36 hours at 130 °C. Overall, the nitrogen-based moieties were demonstrated to influence polymerization kinetics, catalyze the dynamic transesterification exchange mechanism, and aid in the solvolysis of the thermosets at end-of-life.

Introduction.

Crosslinked polymers, or thermosets, comprise 12-20% of annual plastics production of which rigid thermosets, those with high glass transition temperature (T_g), are commonly employed as a matrix polymer in reinforced composite technologies for automotive, construction, industrial, automotive, and other energy-dependent applications. Currently, epoxy-amines are the industry standard for glassy thermosets due to their simple bulk curing preparation coupled with robust thermomechanical properties. Specifically, the dense and highly cross-linked network architecture affords thermosets with chemical resistance, thermal stability, and strength. Consequently, these same characteristics make these materials recalcitrant to conventional recycling strategies, limiting or nullifying end-of-life options for material recovery.¹⁻³

This lack of recyclability has motived a large amount of research into polymer systems with covalently adaptable networks (CANs), also referred to as vitrimers, that are specifically designed for reversible bond exchange that can enable chemical recycling or melt-like reprocessability, even in thermosetting networks. The bond exchange chemistries are triggered by a range of external stimuli (light, pressure, temperature, etc.). When exchange is triggered, the rearrangement of the network topology allows for sufficient mobility to emulate flow and achieve reprocessability. Importantly, when stimulus is not present, the bond exchange is significantly slowed, imparting crucial thermoset rigidity. Epoxy-anhydride polyester thermosets are a widely studied CAN platform, capable of leveraging the ester repeat unit, from the anhydride hardener, as a recyclability handle. Additionally, when formulated properly to ensure an excess of hydroxyl groups, polyester covalent adaptable networks (PECANs) can be susceptible to transesterification for dynamic bond exchange in addition to solvent-mediated deconstruction chemistries (e.g. hydrolysis, methanolysis, etc.). It is important to note that the epoxy-anhydride polymerization to produce PECANs does require the use of a catalyst, routinely ~1 wt.% tertiary amine moiety, to initiate the polymerization. Generally increasing this loading leads to reduced curing inputs while hindering network architecture and thermomechanical performance.

In 2011 Montarnal *et al.* first reported on rigid polyester vitrimers demonstrating the advantages of in-network transesterification for fully reprocessable, glassy thermosets from epoxy-acid and epoxy-anhydride precursors.⁴ External addition (5 – 10 mol %) of zinc acetate, however, was required to observe feasible flow behavior otherwise inaccessible through the initial 0.1 mol % Zn loading. Since this discovery, a variety of developments have been made in enhancing the means of transesterification in PECAN materials.⁵⁻⁹ One of the more intriguing examples of enhancing transesterification was reported by Altuna *et al.* where they leveraged relatively high loadings of butylamine and di-butylamine bound into the network as tertiary amines following epoxide ring-opening initiation.¹⁰ The covalent incorporation of the amine units presented an opportunity for an internal, embedded nucleophile to catalyze transesterification reactions. The above consideration highlights that the role of the amine catalyst is not limited to polymerization and can also catalyze important dynamic exchange reactions found in PECAN architectures through nucleophilic action.

As the role of the tertiary amine efficacy in the triple catalytic action of polymerization, transesterification, and deconstruction is still not known, we set forth to understand this effect as a function of catalyst chemistry and structure. Specifically, we selected 12 tertiary amines spanning aliphatic, amidine, and R₆ aromatic (R = C/N) classes with varying sterics and electronic environments. Tertiary amines were selected for this study because they are demonstrated to exhibit facile anionic polymerization mechanisms.¹¹⁻¹⁴ We first demonstrate the role of the amine moiety in the epoxy ROCOP by comparing the polymerization of a model thermoplastic epoxy-amine and epoxy-anhydride system through hydrogen nuclear magnetic resonance (¹H NMR) studies. Subsequently, amine-catalyzed PECAN curing events are tracked by differential scanning calorimetry (DSC) at industrially relevant conditions. Finally, we evaluate the effectiveness of the internal catalysts to promote transesterification by rheological stress relaxation (reprocessing) and methanolysis deconstruction. Overall, all selected catalysts show increased efficacy in curing and dynamic exchange over the uncatalyzed system, and the experimental results are coupled with analysis of the amine structure towards the development of structure-function principles that drive the reported triple-catalytic action.

Results.

Model ROCOP *in situ* NMR studies. Prior to any catalyst screening studies, we sought to understand the polymerization mechanism of the epoxy-anhydride (E-Anh) system. Specifically, as PECANs are commonly justified as a replacement for epoxy-amine (E-Ami) systems, we wanted to understand the differences between these two polymerization pathways. For this study, model thermoplastic systems were devised to allow for *in situ* solution-state NMR spectroscopic monitoring. These systems are amenable to *in situ* kinetics NMR because the polymer T_g remains below 80 °C during initial polymerization, maintaining molecular mobility required for solution-state NMR signal observability. In addition to quantitative ^1H kinetics monitoring, the high sample concentration (~10 M) allowed rapid acquisition of ^{13}C and 2D HSQC spectra, providing detailed and comprehensive insight into evolving chemical environments during polymerization.

For the E-Ami polymerization, we studied a system consisting of stoichiometric quantities (1:1 molar) of aniline and butanediol diglycidyl ether (BDODGE) that were dissolved in d_8 -toluene and equilibrated at 80 °C before successive ^1H NMR spectra (600 MHz). The reaction was monitored via integration of assigned proton peaks that are consumed or generated throughout the reaction, allowing for the quantification of constituent concentration and reaction rates. The reaction scheme and corresponding proton assignments and color scheme are shown in **Figure 1A** (with spectral overlay given in **Figure S1A**). **Figure 1B** and **1C** provide a time course of the E-Ami polymerization in terms of consumption and rate, respectively. In the E-Ami polymerization, aniline (6.43-6.50 ppm - grey) was initially consumed at twice the rate of BDODGE (2.79-2.93 ppm - blue) with consumption rates of ~9.7 and ~5 $[\mu\text{M}]/\text{s}$ for the first 6 hours, respectively. This suggested that the reaction rate is first order in the epoxy and second order in the amine which was further corroborated with the presence of the di-amino trimer intermediate species (3.80-3.90 ppm - orange) depicted in **Figure 1A**. A reaction mechanism is proposed in **Figure S2**. In strong support, both aromatic and oxygenated aliphatic C-H signals assigned to the proposed intermediate are captured in the time-course 2D HSQC data (**Figure S1C**). Once the concentration of the intermediate peaks after 12-18 hours, the intermediate was then consumed over the next 8 hours with a rate ~twice that of BDODGE (11.1 vs 6.3 $[\mu\text{M}]/\text{s}$) as the trimer linkages are bridged together with BDODGE, and the E-Ami polymer (3.94-4.15 ppm - green) production significantly increases, consistent with step-growth kinetics. After 36 hours, the reaction is significantly slowed (< 2.5 $\mu\text{M}/\text{s}$) which was attributed to solvation limitations, gelation, or vitrification.

For the E-Anh polymerization, stoichiometric (1:1 molar) methylhexahydrophthalic anhydride (MHHPA) was combined with phenyl glycidyl ether (PGE) in d_8 -toluene with 0.02 molar equivalent (~1wt%) of N-methyl piperidine (MPip) as the reaction catalyst. Similarly, the reaction scheme and corresponding proton assignments studied are presented in **Figure 1D** (with a spectral overlay given in **Figure S1B**). As shown in **Figure 1E**, the E-Anh reaction proceeds significantly faster than the model E-Ami reaction as PGE (3.60-3.73 ppm - brown) and MHHPA (2.72-2.87 ppm - purple) were consumed at a rate of 397 and 523 $[\mu\text{M}]/\text{s}$ (**Figure 1F**), respectively. Importantly, MHHPA is consumed at a faster rate than PGE, which suggests that MPip catalyst initially attacked the anhydride carbonyl. A reaction mechanism is proposed in **Figure S3**. After a sharp increase in consumption of both monomers, the monomer consumption rates became equivalent as the alternating ROCOP continued. The E-Anh polymer product (5.18-5.46 ppm - red) continued to grow, consistent with a chain-growth mechanism until polymerization slows which can again be attributed to limitations of the experiment. When all MHHPA is consumed, PGE continues to react. This phenomenon is could be attributed to homo-polymerization or etherification as documented by others.^{11, 13, 14} A mechanism of this side-reaction is proposed in **Figure S4**.

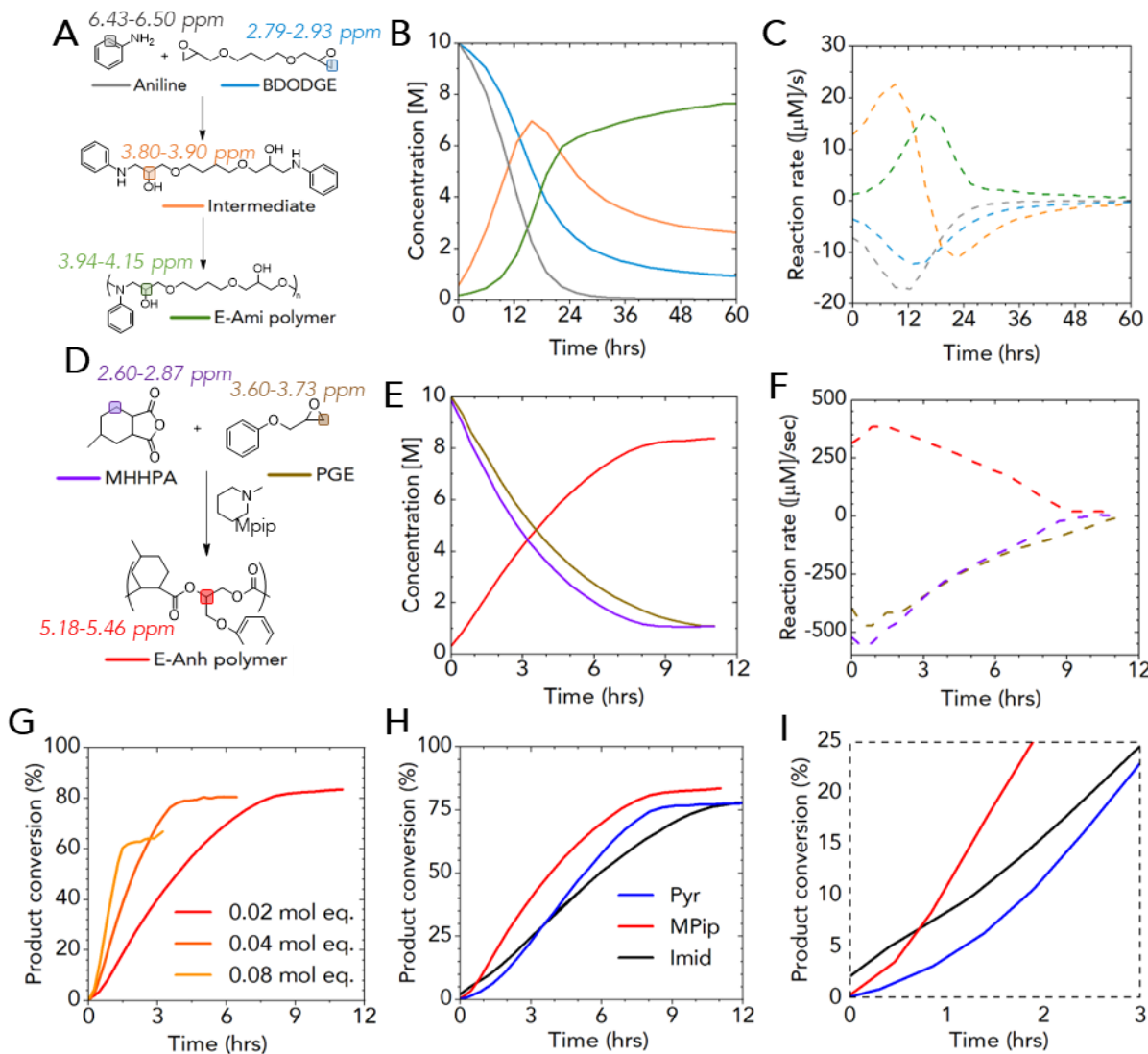


Figure 1. Epoxy ring opening polymerization mechanism studied via ^1H NMR. **A.** Model ^1H NMR E-Ami reaction of aniline (6.43–6.50 ppm) with BDODGE (2.79–2.93 ppm) to generate a secondary intermediate species (3.80–3.90 ppm) before E-Ami polymer (3.94–4.15 ppm) conversion. The spectral overlay, with corresponding assignments, is provided in **Figure S1**. **B.** Calculated BDODGE (blue), aniline (grey), secondary amine intermediate (orange), and E-Ami polymer (green) concentrations from corresponding integrations over time. **C.** Derived reaction rates for E-Ami experiment with respect to time. **D.** Model ^1H NMR E-Anh reaction of MHHPA (2.60–2.87 ppm, after spectral alignment) with PGE (3.60–3.73 ppm), catalyzed by 0.02 mol eq. MPip, to generate E-Anh polymer (5.18–5.46 ppm) product. The spectral overlay, with corresponding assignments, is provided in **Figure S1**. **E.** Calculated PGE (brown), MHHPA (purple), and E-Anh polymer concentrations from corresponding integrations over time. **F.** Derived reaction rates for E-Anh experiment with respect to time. **G.** Product conversion, normalized by initial concentration of MHHPA, for the E-Anh polymer at 0.02, 0.04, and 0.08 mol eq. of MPip catalyst loading. **H.** Product formation of E-Anh polymer, normalized by initial concentration of MHHPA, from 0.02 mol eq. of MPip (red), Pyr (blue), and Imid (black). **I.** Inset of E-Anh polymer formation depicted in **H** over the initial 3 hours.

We then sought to gain a preliminary understanding of the effect of catalysts on this model system prior to its exploration in application relevant thermosetting PECAN systems. To start, the role of MPip in the E-Anh reaction profile is further explored at higher catalyst loadings of 0.04 eq. and 0.08 eq. (**Figure 1G**). As expected, increasing the loading of the initiating catalyst promotes accelerated product formation wherein 0.08 mol eq. of MPip product yields nominal ($>60\%$) product formation after 3 hours. However, polymerization appeared to be stunted by this increased loading which can be attributed to higher, non-stoichiometric consumption of the anhydride, highlighting the delicate balance of catalyst loading. After consumption of the anhydride, etherification is expected to nominally take place, albeit much slower, at longer reaction times that were not tested.

Finally, the role of the amine catalyst was further explored by incorporating other catalysts into the model E-Anh system described above. Specifically, an amidine catalyst, imidazole (Imid), and an R₆ aromatic (R refers to carbon

or nitrogen containing 6 membered rings) catalyst, pyridine (Pyr), were polymerized and polymer conversion profiles are shown in **Figure 1H**. At a 0.02 mol eq. loading, all three catalysts yield nominal conversion after 9 hours. Interestingly, all three reactions exhibit a small incubation period (0-3 hours) of regressed product formation before linear growth of the polymer (**Figure 1I**). Specifically, the MPip catalyzed reaction accelerates after 0.5 hours while the Imid and Pyr reaction begins a muted acceleration after 2 hours, each at different rates. Overall, the identity of the amine catalyst plays a role in E-Anh product formation that can inform processing parameters of a thermosetting system and merits further research.

PECAN curing phenomenon. We further explored the role of the catalyst in the polymerization of E-Anh networks, by leveraging an industrially relevant thermosetting PECAN system with backbone ester and hydroxyl functionality, previously studied by our group. Specifically, we choose a PECAN network that was comprised of 0.7 mol eq. of BDODGE, 0.3 mol eq. sorbitol polyglycidyl ether, and 1.0 mol eq. of MHHPA.^{15, 16} In addition to the catalysts studied above, 9 additional catalysts, spanning the three subdivided classes, were added to the scope of this study for a thorough understanding of structure-property relationships for PECAN polymerizations. In addition to MPip, the aliphatic amines triethylamine (TEA), tripropylamine (TPA), and tributylamine (TBA) were studied. In addition to Imid, the amidines of 1-methyl imidazole (1MI), 2-ethyl-4-methyl imidazole (24EMI), and 1,8-Diazabicyclo[5.4.0]undec-7-ene (DBU) were studied. In addition to Pyr, 3 more R₆ amine derivatives were studied; dimethylaniline (DMA), 4-dimethylaminopyridine (DMAP), and N,N,N,N-tetramethyl-1,4-phenylenediamine (TMEDA). The structures of the catalysts studied are given in **Figure 2A**.

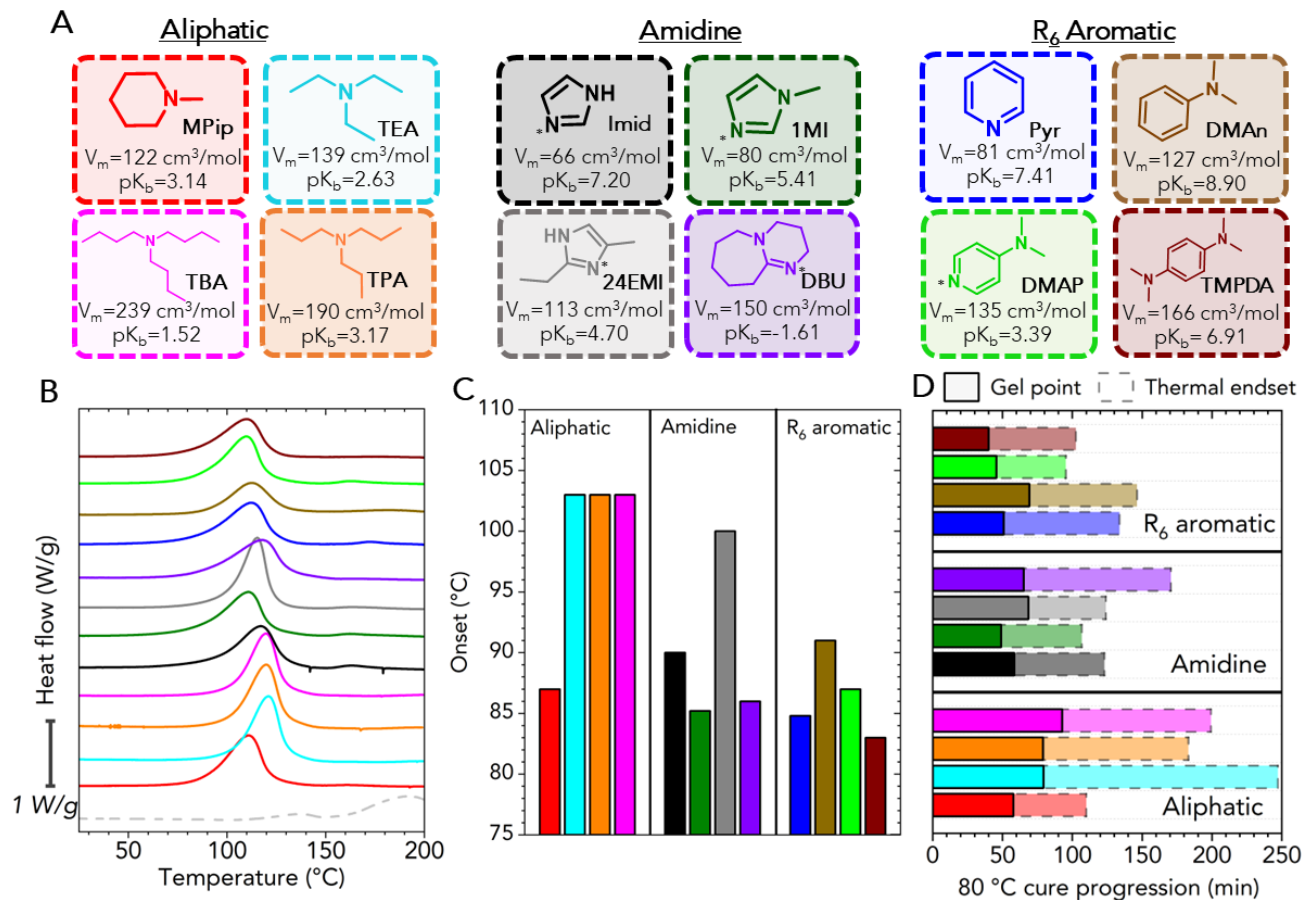


Figure 2. Tertiary amine catalyzed PECAN polymerization. **A.** Chemical structure, molar volume (V_m), and calculated pK_b for all 12 catalysts studied segregated by chemical class (aliphatic, amidine, and R₆ aromatic) and color. **B.** DSC temperature ramping ($2\text{ }^{\circ}\text{C}/\text{min}$) thermograms of PECAN resins overlaid and color coordinated. The uncatalyzed reaction is depicted in a dotted and light grey curve. **C.** Onset of cure temperatures are quantified with color coordination for each catalyst from DSC dynamic cures. **D.** Gelation points of PECAN resins with various catalysts were quantified by rheology experiments ($80\text{ }^{\circ}\text{C}$, 1% strain, 10 rad/s) as the storage and loss modulus crossover and are presented in solid, color coordinated bars. Additionally, reaction endset times were determined from DSC isothermal experiments at $80\text{ }^{\circ}\text{C}$ and are presented in semi-transparent, dashed, and color coordinated bars. Individual rheological graphs are given in **Figure S6** and individual DSC isothermal thermograms are given in **Figure S7**. Onset temperatures, gel points, and endset temperatures are tabulated in **Table S2**.

Catalysts were selected due to their different structures to enable the elucidation of structure-property relationships. Specifically, we expected that the primary factors to contribute to the efficacy of the tertiary amine to act as a nucleophile in the epoxy thermoset polymerization are basicity and steric hindrance. To address the former, we predicted the relative basicity of the various tertiary amine catalysts via determination of pK_b . For this study, we utilized a refined version of novel computational, DFT-based, method¹⁷⁻¹⁹ that demonstrated high accuracy in predicting the pK_b of primary amines.²⁰ We calculated the pK_b at 25 °C for the 12 PECAN catalysts utilizing three explicit water molecules at the reaction center. A diagram of the coordination environment is exemplified in **Figure S5** for TEA (and its protonated analog, triethylammonium) and calculated values are tabulated in **Table S1** with some comparisons to those found experimentally. While the calculated pK_b 's show good agreement with those found in literature, it is important to acknowledge that our calculations are made with three explicit water molecules and fail to account for the complex solvent environment of bulk experimentation. Further details on the computational methodology are reported in the Methods section. In addition to the pK_b 's, molar volume was also calculated from each molecule's molar mass (NIST) and density (CRC) to gauge steric hindrance. Both molar volume and the pK_b 's for each catalyst are shown in **Figure 2A** with their corresponding structure, abbreviation, and color coordination used throughout this report.

With a basic understanding of the molar volumes (V_m) and catalyst basicity, we applied these metrics to the PECAN resin. Specifically, liquid PECAN resins with 0.02 mol eq. of studied catalyst were combined and subject to differential scanning calorimetry (DSC) curing experiments. The thermosetting solution was dynamically cured within a DSC at 2 °C/min to garner the thermal response of each system as a function of temperature. Dynamic cures for each catalyst are overlayed and shown in **Figure 2B** for all 12 catalysts as well as the uncatalyzed PECAN system (dashed grey line). The total exotherm of the reactions with respect to temperature were conserved (360 ± 20 J/g) as the total molar quantity of reactive groups were held constant.

For each catalytic system we studied the thermodynamic barrier to polymerization that we correlated as the onset temperature. The onset temperature was calculated as the temperature when the exotherm begins to dramatically increase and is presented in **Figure 2C** as a bar chart. Without catalyst, the PECAN resin exhibits a complex curing profile with two shallow peaks that do not significantly exotherm until temperatures > 150 °C. Conversely, the catalyzed PECAN resins exhibit monomodal cure behavior at lower temperatures. Specifically, among the aliphatic series, MPip exhibits the lowest V_m and comparable pK_b (within an order of magnitude), suggesting that it will be a strong nucleophile which is supported by an onset temperature lower than the other studied aliphatic amines (87 °C vs. 103 °C). Comparing imidazole to its derivations also leads to some structure property relationships. For example, replacing a proton with a methyl group (from Imid to 1MI) marginally increases the size of the catalyst, however the ensuing reduction in pK_b (7.20 to 5.41) could be responsible for the reduction in onset temperature (90 °C vs. 85 °C). The addition of a methyl and ethyl group to the imidazole ring (24EMI) increases the basicity of the catalyst further, however the ensuing steric hindrance resulted in an onset temperature of 10 °C higher than that of Imid. Despite the bulkiness of the chemical structure, DBU exhibits one of the lowest onset temperatures which is owed to the appreciably low pK_b (-1.61) and unencumbered amine site. Similar relationships can be made by comparing pyridine derivatives. Compared to Pyr, DMAAn is much bulkier, specifically hindered by the nitro-methyl groups and consequently did not initiate until 6 °C higher than the Pyr analog. Appropriately, DMAP exhibited a lower initiation temperature than DMAAn, owed to the unencumbered active site as well as the appreciably lower pK_b (3.39 vs. 8.90). Within this study TMPDA exhibited the lowest onset temperature that can be attributed to 2 equivalent and basic nitrogen active sites that circumvent expected steric limitations inherent to the dimethyl groups. This observation highlights not only the importance of basicity on curing initiation, but also the quantity of the active sites within the catalyst structure which play a pivotal role in catalyst efficiency.

The DSC experiments provided insight into the thermodynamic consequences of catalyst choice, but the 3-dimensional PECAN network will also be subject to kinetic limitations that, too, could be artifacts of catalyst identity. Therefore, rheological and additional thermal studies were conducted to understand the efficacy of the monomers to solidify and complete polymerization of the network which can inform crucial processing parameters for industry relevance. Specifically, an oscillatory (1% strain, 10 rad/s), isothermal (80 °C) rheological experiment was performed on all PECAN formulations to determine the gelation (gel) point which was determined as the crossover point of the storage and loss modulus. The reaction temperature was methodically chosen as it is industrially relevant and below the thermal barrier to polymerization of all tested mixtures. In tandem to these experiments, the PECAN mixtures

were cured isothermally at 80 °C within a DSC to thermally evaluate the completion of the reaction; quantified here as the reaction endset, or the time when the exotherm begins to drastically reduce. Both gel point (solid fill) and endset (semitransparent, dashed border) are depicted in **Figure 2D** in color coordinated fashion.

Most of these polymerization metrics follow similar trends to the onset temperature calculations (**Figure 2C**) which can be attributed to the explanations above for the role of the nucleophilic catalyst. However, TEA surprisingly exhibits the longest endset temperature (247 minutes) despite having a similar gel point to its propylated derivative (79 minutes). This observation is attributed to the volatility of TEA ($T_{boiling}=89$ °C) where the catalyst could volatilize over the course of the slow reaction resulting in diminished curing efficiency. Within the amidine series, the curing efficacy of DBU is thwarted by the bulky nature of the molecule ($V_m = 150$ cm³/mol) resulting in an extended thermal and rheological curing profile compared to the other amidine derivates as well as the trends observed for onsetting temperature. As evident from the curing profile of TMPDA ($V_m = 166$ cm³/mol), the employ of multiple, equivalent nitrogen active sites can circumvent this artifact as TMPDA completes the cure well before DBU (103 min. vs. 171 min.). Taken together, we assert that tertiary amines follow expected characteristics of a nucleophile in the polymerization of epoxy-anhydride systems but exhibit diffusion limitation effects in a thermosetting network.

PECAN Transesterification. After elucidating structure property relationships for the role of the catalyst in polymerization of a PECAN system, we sought to determine the efficacy of the now internal amine catalyst in transesterification (**Figure 3A**). To these ends, PECAN resin mixtures were cast into desired geometries and cured isothermally at 80 °C for 5 hours and then post-cured at 180 °C for 1 hour, to ensure the reaction of all functional groups. Stress relaxation experiments within a dynamic mechanical analyzer (DMA) were used to quantify the transesterification of cured PECAN resins. Within these experiments, the PECAN resins are loaded in a single cantilever geometry and heated to 200 °C at which point a 0.25% strain is applied and modulus is measured. Over a 5-hour experiment, the bond exchange will enable the network to reconfigure into this strained environment, exemplified in a reduction of modulus. The modulus is normalized to time zero and reported in **Figure 3B**.

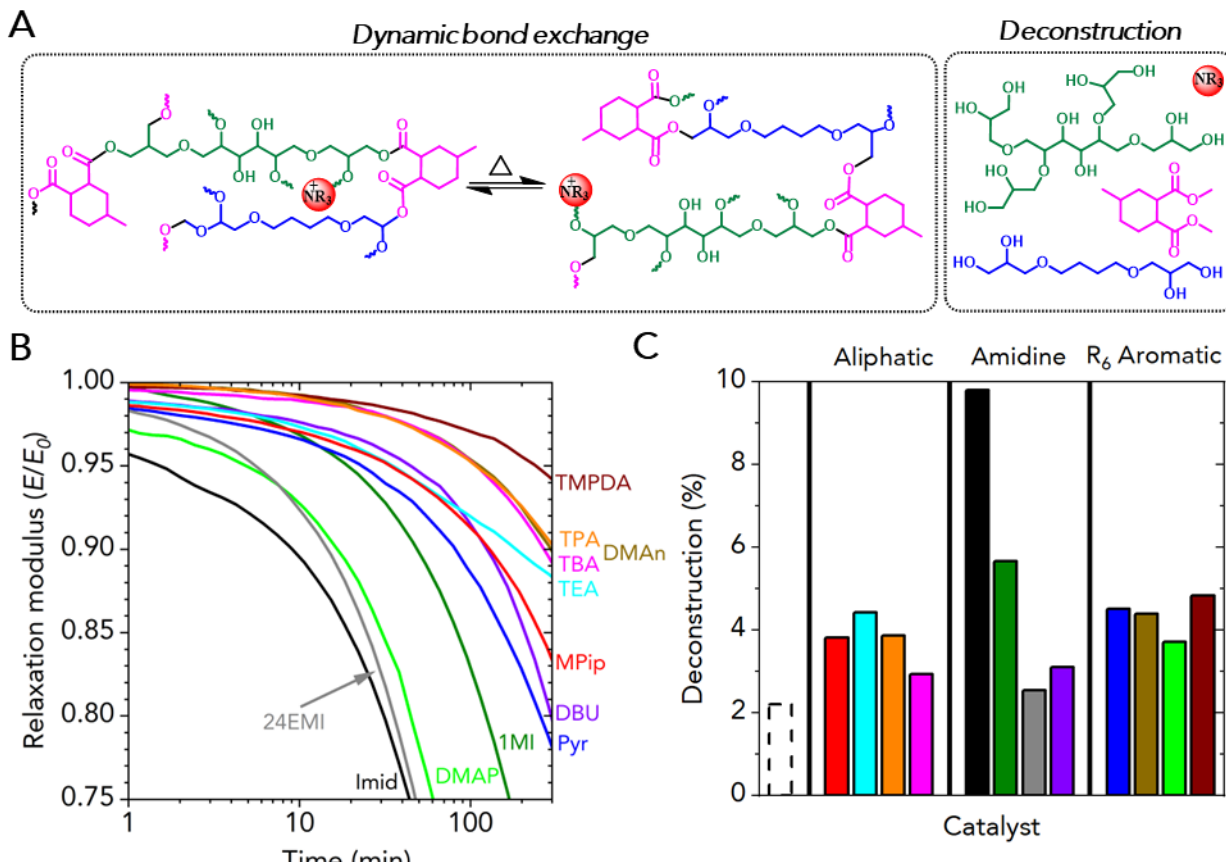


Figure 3. Catalyzed covalent adaptable network rearrangement. **A.** Abbreviated reaction scheme for internal transesterification (left) and depiction of methanolysis products (right). **B.** Overlay of DMA stress relaxation experiments (200 °C, 0.25% strain, 5 hour) performed on cured PECAN resin bars. The full relaxation profiles are given in **Figure S8**. **C.** Bar charts depicting normalized mass loss (depicted as

deconstruction) after 130 °C methanolysis experiments (36 hours, 5mL methanol/g PECAN). The dotted bar represents the deconstruction of a PECAN thermoset disk without an internal catalyst. The deconstruction data is also presented in **Table S3**.

Within a highly crosslinked PECAN network, the efficacy of the bound catalyst is expected to be severely diminished because of the reductions in diffusion potential. This hypothesis is supported where the larger, bulkier aliphatics of TEA, TPA, and TBA exhibited reduced relaxation efficiencies compared to MPip. Within the R₆ aromatic series, PECAN with DMAP exhibited the fastest relaxation which is counter-intuitive to this theory and merits future research. However, the other thermosets cured with R₆ aromatics showed expected relaxation profiles based on their molar volume where Pyr ($V_m = 81 \text{ cm}^3/\text{mol}$) exhibited 82% relaxation, DMA_n ($V_m = 127 \text{ cm}^3/\text{mol}$) exhibited 90% relaxation, and TMPDA ($V_m = 166 \text{ cm}^3/\text{mol}$) showed 94% relaxation over 300 minutes. Overall, the amidines, and especially the imidazoles, exhibited the fastest relaxation of the tested catalyst sub-sets which is likely attributed to the reduced size of the imidazole family having a better propensity to diffuse into the network. Specifically, Imidazole showed 75% relaxation over 45 minutes. Within this subset, DBU ($V_m = 150 \text{ cm}^3/\text{mol}$) still showed accelerated relaxation compared to other catalysts with similar volume. Overall, the catalyst used for curing the PECAN polymer was found to also assist in bond exchange.

Finally, the ability of the internal amine catalysts to aid in external transesterification with methanol (methanolysis) was explored. Cured PECAN disks (12mm diameter, 7mm thick) were polymerized with alternative catalysts as described above and subsequently added to methanol (5mL/g) into a high-pressure glass vial at 130 °C for 36 hours without external catalyst. From previous work, the PECAN deconstruction can take place without external catalyst within 6 hours at 225 °C, therefore this reaction temperature was chosen to elicit variable deconstruction behavior allowing for the quantification of trends. The mass loss (% deconstruction) was then calculated with results presented in **Figure 3C**. In all cases, the catalyzed PECAN thermosets deconstructed to a greater extent than the uncatalyzed analog which emphasized the beneficial role of the nitrogen moiety in this reaction. Clear trends are observed from the aliphatic series, particularly among the linear alkanes where the smaller TEA catalyst has greater efficiency in the deconstruction than the TPA and TBA analogs (4.42% vs. 3.86% vs. 2.94%). Corroborating the stress relaxation experiments, Imid was the most efficient deconstruction catalyst (9.8%) owing to the small size and labile nitrogen positioning. Surprisingly, PECAN polymer cured with 24EMI exhibited the least amount of deconstruction in this experiment, contrasting the observed stress relaxation profile. This anomaly could be attributed to the ethyl group alpha to both nitrogens disrupting coordination but requires further investigation. Unfortunately, the deconstruction of the R6 aromatic set exhibited a tight variance ($s^2=0.22\%$) and meaningful conclusions could not be made. To garner a more differentiable difference in deconstruction efficacy, a secondary experiment was conducted from a method previously reported by Wang et al.¹⁵ Specifically, select alternatively catalyzed PECAN thermosets from each subgroup were subjected to methanol (10mL/g) within standard 20mL scintillation vials at 65 °C for 48 hours. In this case, 5wt% (relative to PECAN mass) of potassium carbonate catalyst was used to accelerate deconstruction. The results of this experiment are depicted in **Figure S9**. The same trends, albeit on a larger scale (>8x higher deconstruction efficacy), are observed in this deconstruction experiment (Method B), when compared to the above experiment (Method A). Importantly, all thermosets deconstructed more than the uncatalyzed counterpart. PECAN thermosets cured with TEA deconstructed more than the aliphatic analog MPip (42% vs. 26%) and those cured with 1MI deconstructed to a greater extent than 24EMI (46% vs. 27%), corroborating the above observations and interpretations from **Figure 3C**. Again, the R₆ aromatic amine catalysts were not found to exhibit significantly different deconstruction efficacy. Overall, the electronics and more importantly, the structure of the catalyst used to cure the PECAN resin also offers the ability to catalyze dynamic exchange mechanisms after crosslinking.

Discussion.

Epoxy-amine systems belong to the most commercially available thermosetting polymer systems available and consequently have been studied for decades.²¹ The reaction mechanism for the thermosetting systems, as well as thermoplastic analogs, have been well documented and are ubiquitously agreed to proceed via autocatalytic, step-growth mechanisms, to which our studied model is in agreement with.²²⁻²⁴ Despite research spanning more than 60 years, the exact mechanism that dictates the polymerization of epoxy-anhydride systems have not been concretely defined. For example, the initiation of these systems has been reported to begin via nucleophilic addition to the oxirane ring, however some reports also show coordination to the anhydride monomer that begins the polymerization. There are even some reports that justify a complex coordination mechanism through hydroxyl activation and eventual ring opening polymerization.^{11, 14, 25-29}

To bolster the industrial relevance of E-Anh thermosets, particularly PECAN thermosets, this work targets a fundamental understanding of the role of the catalyst, not only in ROCOP, but also in the development of a 3-dimensional thermosetting system. To the former point, a model E-Anh reaction, when catalyzed by a tertiary amine moiety (MPip in this study) was found to polymerize in a manner consistent with a chain growth mechanism, contrasting the step growth polymerization of an E-Ami polymer. These observations corroborate the fundamental understanding of the catalyst's role in the polymerization, although the exact mechanism of the tertiary amines catalyst prompts further research. Within a thermosetting, PECAN system the studied catalysts exhibited onsets of polymerizations within a 20 °C range (83-103 °C), gel points within a 50-minute range (40-93 minutes), and cure completions (via thermal endset) within a 153-minute range (95 – 247 minutes) range. All of these experiments were performed at only a 0.02 or ~1wt% loading of catalyst, highlighting the importance of the catalyst in PECAN systems. While these loadings were chosen for industrial relevance, they still require large processing inputs ($T_{cure} \geq 80$ °C, $time_{cure} > 90$ minutes) which can limit their application space to low volume manufacturing. However, a report by Rocks et al. utilized nitro glycidyl ether and anhydride moieties to increase the nitrogen loading (stoichiometric) and consequently observed reaction onset temperatures < 40 °C, validating the efficacy of the nitrogen content.³⁰

In stark contrast to E-Ami thermosets, E-Anh systems can leverage labile ester bonds to enable reprocessing or chemical recycling. Within this report, PECAN resins cured with alternative catalysts show varied stress relaxation responses and deconstruction efficiencies. To that end, it was found that Imid was the most effective catalyst in both processes which is owed to its exuberantly low molar volume ($V_m = 66$ cm³/mol) that affords better diffusion in a densely crosslinked network. However, within this studied system, we acknowledge that >60 minutes for 75% stress reduction is not conducive to thermal processing techniques like extrusion, compression molding, and thermal stamping. Aligned with other observations, increasing the nitrogen content can illicit faster transesterification. Specifically, stoichiometric diamines have been showed to easily react with glycidyl esters generating polyester covalent adaptable networks with stoichiometric nitrogen quantities that, consequently, exhibit melt-like processing.³¹ Almost all reports on PECAN deconstruction techniques leverage external catalyst to increase the efficacy of the deconstruction, however the role of the amine catalyst used for curing has seldom been reported as also being responsible transesterification (via stress relaxation), with known reports showing only the effect of concentration instead of composition.¹³ Therefore, these experiments offer a pivotal platform for future research in recyclable by design thermosets where catalyst designed for curing can also be designed for facile deconstruction or reprocessing.

Conclusion.

Within this work, we utilized ¹H NMR experiments on model E-Ami and A-Anh systems to compare and contrast the different reaction pathways of the epoxy ROCOP with different reactive catalysts, noting the E-Ami system prescribes to a conventional step-growth polymerization while the E-Anh system classifies more to a chain-growth mechanism. Furthermore, the E-Anh polymerization is dependent on the amine-based catalyst concentration and identity. To further this understanding, a total of 12 amine-based catalysts were studied in the thermosetting polymerization of a PECAN thermoset. After quantification of the catalysts' nucleophilic characteristics, the efficacy was determined to follow, for the most part, expected trends in polymerization with some discrepancies noted from molar volume and catalyst volatility. Finally, the same, now internal, catalyst was discovered to play a crucial role in the covalent adaptable nature of the system. However, the expected nucleophilic role of the catalyst was complicated by other factors not explicitly studied, but are grounds for further, more comprehensive studies.

Materials and Methods.

Materials. MHHPA was purchased from Broadview Chemicals. The sorbitol polyglycidyl ether (epoxide equivalent weight – EEW: 179 g/eq) and BDODGE (EEW: 126.4 g/eq) used in the PECAN formulation were purchased from Huntsman. The BDODGE used for the NMR E-Ami model system was purchased from Sigma Aldrich. 24EMI, 1MI, Imid, DBU, TMPDA, Pyr, DMAAn, TEA, TPA, and aniline were also purchased from Sigma Aldrich. d₈-toluene was purchased from Cambridge Isotope Laboratory. MPip was purchased from Thermo Scientific. Methanol was purchased from Fisher Chemical. PGE was purchased from AABlocks. TBA and DMAP were purchased from TCI Chemicals. All chemicals were used as received.

Resin Synthesis. Neat polymer samples were prepared by mixing 0.3 mol eq. of SPGE (17.3 wt%), 0.7 mol eq. BDOGE (28.5 wt%), and 1.0 mol eq. MHHPA (54.2 wt%) at ~20 g scales in plastic polypropylene cups. To this mixture, 0.02 mol of tested catalyst was then added volumetrically (for liquid catalysts) or gravimetrically (for solid catalysts) and the mixture was hand mixed for 2 minutes and then speed mixed at 1000 rotations per minute for 10 seconds and 2000 rotations per minute for 2 minutes. Subsequently, the resin was cast into Teflon molds with a pre-designated geometry [rectangular DMA bars (12mm wide x 60mm long x 2mm thick) or resin disks]. Finally, the PECAN resin was cured in an oven at 80 °C for 5 hours and 180 °C for 1 hour. Uncatalyzed resin samples were cured at 180 °C for 5 hours.

Catalyzed Resin Deconstruction. PECAN resin disks (12mm diameter × 7mm thickness) were fabricated by the above curing protocol utilizing each amine catalyst individually. Pre-weighed, cured and post-cured cubes were placed in a sealed microwave vial with a solution of methanol (5 mL/g of resin) and heated to 130°C, under stirring for 8 hours, cooled to room temperature overnight, and then continued heating for 28 hours. After reaction, the remaining resin was collected by filtration, dried overnight in a vacuum oven (40 °C), and the final mass was recorded.

$$\% \text{ Deconstruction} = \frac{(\text{Recovered PECAN mass})}{(\text{Initial PECAN mass})} \times 100$$

Density functional theory (DFT) calculations for pK_b. All calculations were performed with Gaussian 16.³² DFT calculations for determining pK_b values utilized the CAM-B3LYP functional due to its consolidated reliability in computing pK_b and pK_a.^{17, 18, 20} Solvation model based on density (SMD) was demonstrated as a reliable model in mimicking water as solvent, especially in combination with CAM-B3LYP.²⁰ 6-311 G+(d, p) was selected as basis set for its reliability in describing the geometry of small organic compounds and hydrogen bonds.^{33, 34} Initial geometries were constructed with the goal of achieving a water position as close as possible to ones in solution. Based on previous work unveiling the most stable configuration of water molecules in acid and basic environments,³⁵ three-water molecules were initially placed at the reaction center of the neutral (amine) and protonated (ammonium) species,³⁵ as demonstrated in **Figure S6** for triethylamine (TEA); initial geometries for the other catalyst molecules were built starting from either optimized TEA or piperidine configurations. pK_b values were calculated using a refined version of a novel computational method¹⁷⁻¹⁹ that demonstrated high accuracy in predicting the pK_b of primary amines.²⁰ This method does not use *de facto* corrections but it is able to accurately predict pK_b with low computational cost, utilizing only two explicit water molecules at the reaction center.²⁰ This method involves calculation of the energy difference between the protonated and neutral forms of each catalyst molecule for incorporation into the ionogenic equation pK_b = ΔE_{deprotonation}/2.302*RT + 15.74. According with referenced literature,²⁰ a preliminary computation of the pK_b for the 12 PECAN catalysts in water at 25°C was performed. We found that the errors with the tertiary amines utilized in the present study gave larger mean absolute errors than the primary amines and anilines reported previously. We thus adjusted the methodology to include three explicit water molecules within the reaction. Further details will be presented in a follow-up paper.

In Situ Nuclear Magnetic Resonance Spectroscopy. ¹H NMR kinetics measurements were performed in-situ on a 600 MHz Bruker AV4 NEO NMR spectrometer equipped with a 5 mm BBFO iProbe. Samples were prepared and tightly sealed J-Young NMR tube at room temperature and inserted into the magnet. After room-temperature data were collected, the sample was heated to 80 °C to initiate the polymerization reaction using the default Bruker variable temperature controller (80 °C Nitrogen at 525 L/h flow rate). After reaching target temperature, samples were quickly removed from the magnet, inverted a few times to achieve complete mixing and sample homogeneity, then re-inserted, and a n NMR time series was then executed in Automation in IconNMR including ¹H, ¹³C and 2D ¹H/¹³C

HSQC experiments. Since samples were prepared at high (10 M) concentration, each ¹H NMR spectrum was obtained with a short tip angle of 2 degrees to prevent detector saturation. Acquisition parameters were as follows: for ¹H NMR, 16 scan averages and 4 dummy scans per timepoint, 25 ppm spectral width, 2.2 second acquisition time, and 2.5 second recycle delay (1.5 minutes per spectrum), all with a 2 degree tip angle. ¹³C spectra were obtained with the zgpg30 Bruker pulse sequence using 128 scan averages (6 minutes per spectrum), and HSQC data with the hsqcedetgpsp.3 pulse sequence, 2 scan averages, 256 complex points, and 50% Non Uniform Sampling (10 minutes per spectrum). Further, IconNMR was programmed to throttle on / off sample rotation (20 Hz rotation) during 5 or 10 minute gaps before each ¹H NMR experiments to aid sample mixing throughout the in-situ reaction. Each individual spectra were processed using MestreNova version 15, and kinetics were monitored by tracking assigned and resolved ¹H spectral integrals over time, starting from the first ¹H NMR after sample inversion and re-insertion.

Dynamic Scanning Calorimetry (DSC). A Discovery X3 (TA Instruments) DSC was used for dynamic and isothermal measurements. 10 ± 2 mg of mixed PECAN resin (with or without catalyst) was added to a high volume, o-ring sealed DSC pan. For dynamic curing experiments, the DSC pan was heated at 2 °C/min from 0 °C to 200 °C. For isothermal experiments, the uncured PECAN resin (with or without catalyst) was equilibrated at 80 °C before being isothermally cured at that temperature for 300 minutes. The thermal endset was determined by intersecting tangent lines from the diminishing exotherm and the end of the test.

Dynamic Mechanical Analysis (DMA). A Discovery DMA 850 (TA instruments) was used for stress relaxation experiments. Rectangular bars were fabricated as described above and loaded into the instrument in a single cantilever geometry. The DMA furnace was then heated to 200 °C and 0.25% strain was applied for 5 hours and the modulus was recorded. The relaxation modulus was then normalized to the initial modulus and reported as the Relaxation Modulus (E_0/E).

Oscillatory rheology. A hybrid rheometer – HR20 (TA Instruments) was used for quantification of the gel points for each amine catalyzed PECAN system. Within these tests, ~0.5g of uncured PECAN mixtures were loaded onto 25 mm aluminum disposable plates at room temperature. The plates were then brought together to the trim gap of 1050 μm where excess resin was wiped from the perimeter of the plates. The plates were then closed to the testing gap of 1000 μm before the oscillatory experiment was performed. Within the oscillatory experiment, the plates oscillated at 1% strain and 10 rad/s while being heated at 5 °C/min to 80 °C. At this isothermal temperature, the reaction continued until the storage and loss modulus crossover event was observed.

Supplementary Information (SI).

An SI PDF is provided containing Figures S1-S9, Tables S1-S3, and applicable references.

Data Availability.

All data to reach the necessary conclusions are presented in the main text and SI. Upon reasonable request, the authors will provide additional data.

Author Contributions

Funding Acquisition: NAR

Conceptualization: EGR, RWC, NAR.

Investigation: EGR, RWC, JBA, BCK, NS, SP, AS, LD, LS.

Methodology: EGR, RWC, JBA, BCK, NS, SP, NAR.

Supervision: NAR, BCK

Visualization: EGR, RWC, JBA.

Writing – Original Draft: EGR, RWC, NAR.

Writing – Review & Editing: All authors.

Conflicts of Interest

NAR and EGR have submitted a patent application on recyclable-by-design materials. All other authors declare no competing interests.

Acknowledgements

This work was authored, in part, by the National Renewable Energy Laboratory for the U.S. Department of Energy (DOE) under Contract No. DE-AC36-08GO28308. Funding was provided, in part, by U.S. Department of Energy Office of Energy Efficiency and the Vehicles Technologies Office as well as Grant MUR *Dipartimento di Eccellenza 2023-27 XCHEM* project “eXpanding CHEMistry: implementing excellence in research and teaching”. The views expressed in the article do not necessarily represent the views of the DOE or the U.S. Government. The U.S. Government retains and the publisher, by accepting the article for publication, acknowledges that the U.S. Government retains a nonexclusive, paid-up, irrevocable, worldwide license to publish or reproduce the published form of this work, or allow others to do so, for U.S. Government purposes.

S.P. thanks the Ministero dell’Università e della Ricerca for funding (PRIN 2022 PROMETEO2022KPK8WM project). S.P. thanks the CINECA ISCRA C HP10CKJGZ2.

References

(1) Morici, E.; Dintcheva, N. T. Recycling of thermoset materials and thermoset-based composites: challenge and opportunity. *Polymers* **2022**, *14* (19), 4153.

(2) Zhao, X.; Long, Y.; Xu, S.; Liu, X.; Chen, L.; Wang, Y.-Z. Recovery of epoxy thermosets and their composites. *Materials Today* **2023**, *64*, 72-97.

(3) Jehanno, C.; Sardon, H. Dynamic polymer network points the way to truly recyclable plastics. Nature Publishing Group UK London: 2019.

(4) Montarnal, D.; Capelot, M.; Tournilhac, F.; Leibler, L. Silica-like malleable materials from permanent organic networks. *Science* **2011**, *334* (6058), 965-968.

(5) Debnath, S.; Kaushal, S.; Ojha, U. Catalyst-Free Partially Bio-Based Polyester Vitrimers. *ACS Applied Polymer Materials* **2020**, *2* (2), 1006-1013.

(6) Li, P.; Zhang, X.; Yang, Q.; Gong, P.; Park, C. B.; Li, G. Sustainable polyester vitrimer capable of fast self-healing and multiple shape-programming via efficient synthesis and configuration processing. *Journal of Materials Chemistry A* **2023**, *11* (20), 10912-10926, 10.1039/D3TA00302G.

(7) Lemouzy, S.; Cuminet, F.; Berne, D.; Caillol, S.; Ladmiral, V.; Poli, R.; Leclerc, E. Understanding the Reshaping of Fluorinated Polyester Vitrimers by Kinetic and DFT Studies of the Transesterification Reaction. *Chemistry – A European Journal* **2022**, *28* (48), e202201135.

(8) Berne, D.; Cuminet, F.; Lemouzy, S.; Joly-Duhamel, C.; Poli, R.; Caillol, S.; Leclerc, E.; Ladmiral, V. Catalyst-Free Epoxy Vitrimers Based on Transesterification Internally Activated by an α -CF₃ Group. *Macromolecules* **2022**, *55* (5), 1669-1679.

(9) Guerre, M.; Tapan, C.; Winne, J. M.; Du Prez, F. E. Vitrimers: directing chemical reactivity to control material properties. *Chemical Science* **2020**, *11* (19), 4855-4870, 10.1039/D0SC01069C.

(10) Altuna, F. I.; Hoppe, C. E.; Williams, R. J. J. Epoxy vitrimers with a covalently bonded tertiary amine as catalyst of the transesterification reaction. *European Polymer Journal* **2019**, *113*, 297-304.

(11) Woo, E.; Seferis, J. Cure kinetics of epoxy/anhydride thermosetting matrix systems. *Journal of Applied Polymer Science* **1990**, *40* (7 - 8), 1237-1256.

(12) Amirova, L. R.; Burilov, A. R.; Amirova, L. M.; Bauer, I.; Habicher, W. D. Kinetics and mechanistic investigation of epoxy-anhydride compositions cured with quaternary phosphonium salts as accelerators. *Journal of Polymer Science Part A: Polymer Chemistry* **2016**, *54* (8), 1088-1097.

(13) Tanaka, Y.; Kakiuchi, H. Study of epoxy compounds. Part I. curing reactions of epoxy resin and acid anhydride with amine and alcohol as catalyst. *Journal of Applied Polymer Science* **1963**, *7* (3), 1063-1081.

(14) Matějka, L.; Lövy, J.; Pokorný, S.; Bouchal, K.; Dušek, K. Curing epoxy resins with anhydrides. Model reactions and reaction mechanism. *Journal of Polymer Science: Polymer Chemistry Edition* **1983**, *21* (10), 2873-2885.

(15) Wang, C.; Singh, A.; Rognerud, E. G.; Murray, R.; Musgrave, G. M.; Skala, M.; Murdy, P.; DesVeaux, J. S.; Nicholson, S. R.; Harris, K. Synthesis, characterization, and recycling of bio-derivable polyester covalently adaptable networks for industrial composite applications. *Matter* **2024**, *7* (2), 550-568.

(16) Clarke, R. W.; Rognerud, E. G.; Puente-Urbina, A.; Barnes, D.; Murdy, P.; McGraw, M. L.; Newkirk, J. M.; Beach, R.; Wrubel, J. A.; Hamernik, L. J. Manufacture and testing of biomass-derivable thermosets for wind blade recycling. *Science* **2024**, *385* (6711), 854-860.

(17) Pezzola, S.; Knott, B.; Schultz, N.; Galloni, P.; Sabuzi, F. **manuscript in preparation**.

(18) Pezzola, S.; Tarallo, S.; Iannini, A.; Venanzi, M.; Galloni, P.; Conte, V.; Sabuzi, F. An Accurate Approach for Computational pKa Determination of Phenolic Compounds. *Molecules* **2022**, *27* (23), 8590.

(19) Pezzola, S.; Venanzi, M.; Galloni, P.; Conte, V.; Sabuzi, F. Easy to Use DFT Approach for Computational pKa Determination of Carboxylic Acids. *Chemistry – A European Journal* **2024**, *30* (1), e202303167.

(20) Pezzola, S.; Venanzi, M.; Conte, V.; Sabuzi, F.; Galloni, P. New Insights in the Computational pKb Determination of Primary Amines and Anilines. *ChemPhysChem* **2024**, *25* (17), e202400550.

(21) Pham, H. Q.; Marks, M. J. Epoxy resins. *Ullmann's Encyclopedia of Industrial Chemistry* **2000**.

(22) Mijovic, J.; Wijaya, J. Reaction kinetics of epoxy/amine model systems. The effect of electrophilicity of amine molecule. *Macromolecules* **1994**, *27* (26), 7589-7600.

(23) Foster, J. C.; Yoon, A.; Lyons, K.; Martinez, E. J.; Leguizamon, S. C.; Bezik, C. T.; Frischknecht, A. L.; Redline, E. M. Unexpected Thermomechanical Behavior of Off-Stoichiometry Epoxy/Amine Materials. *Macromolecules* **2023**, *56* (8), 3183-3194.

(24) Birkner, M.; Schreiter, K.; Trommler, K.; Seifert, A.; Spange, S. Ternary hybrid material formation by twin polymerization coupled with the bis-epoxide/amine step growth polymerization. *Polymer* **2017**, *121*, 38-45.

(25) Ding, J.; Peng, W.; Luo, T.; Yu, H. Study on the curing reaction kinetics of a novel epoxy system. *Rsc Advances* **2017**, *7* (12), 6981-6987.

(26) Park, W. H.; Lee, J. K.; Kwon, K. J. Cure Behavior of an Epoxy-Anhydride-Imidazole System. *Polymer Journal* **1996**, *28* (5), 407-411.

(27) Kolář, F.; Svitilova, J. Kinetics and mechanism of curing epoxy/anhydride systems. *Acta Geodyn. Geomater* **2007**, *4* (3), 85-92.

(28) Fisch, W.; Hofmann, W.; Koskikallio, J. The curing mechanism of epoxy resins. *Journal of Applied Chemistry* **1956**, *6* (10), 429-441.

(29) Hesabi, M.; Salimi, A.; Beheshty, M. H. Development of amine-based latent accelerator for one-pot epoxy system with low curing temperature and high shelf life. *European Polymer Journal* **2019**, *112*, 736-748.

(30) Rocks, J.; George, G. A.; Vohwinkel, F. Curing kinetics and thermomechanical behaviour of co-anhydride cured aminoglycidyl epoxy resins. *Polymer International* **2003**, *52* (11), 1758-1766.

(31) Sun, Y.; Wang, M.; Wang, Z.; Mao, Y.; Jin, L.; Zhang, K.; Xia, Y.; Gao, H. Amine-Cured Glycidyl Esters as Dual Dynamic Epoxy Vitrimers. *Macromolecules* **2022**, *55* (2), 523-534.

(32) *Gaussian 16 Rev. C.01*; Wallingford, CT, 2016. (accessed).

(33) Wiberg, K. B. Basis set effects on calculated geometries: 6-311++G** vs. aug-cc-pVDZ. *Journal of Computational Chemistry* **2004**, *25* (11), 1342-1346.

(34) Sabuzi, F.; Stefanelli, M.; Monti, D.; Conte, V.; Galloni, P. Amphiphilic Porphyrin Aggregates: A DFT Investigation. *Molecules* **2020**, *25* (1), 133.

(35) Gillan, M. J.; Alfè, D.; Michaelides, A. Perspective: How good is DFT for water? *The Journal of Chemical Physics* **2016**, *144* (13).